A Three-Dimensional Angle-Optimized Finite-Difference Time-Domain Algorithm

Shumin Wang and Fernando L. Teixeira

***Abstract*—We present a three-dimensional finite-difference time-domain (FDTD) algorithm to minimize the numerical dispersion error at preassigned angles. Filtering schemes are used to further optimize its frequency response for broad-band simulations. A stability analysis of the resulting FDTD algorithm is also provided. Numerical results show that the dispersion error around any preassigned angle can be reduced significantly in a broad range of frequencies with small computational overhead.**

***Index Terms*—Finite-difference time-domain (FDTD) method, numerical dispersion, optimization.**

I. Introduction

NUMERICAL dispersion constitutes a major source of error in the finite-difference time-domain (FDTD) method [1]–[3]. In ordinary FDTDs (Yee's scheme), the numerical dispersion error is maximum along the three coordinate axes [2] and minimum along the cell diagonals. To combat numerical dispersion, it is customary to use finer discretizations or higher order schemes [4]–[12]. These solutions are designed to improve the dispersion properties for all propagation angles simultaneously and demand a significant increase in the computation resources. For a number of practical problems, however, the reduction of the dispersion error is really necessary only around a limited angular sector. This is particularly true, for instance, in (electrically large) problems involving highly elongated FDTD domains and/or problems involving wave propagation limited to certain preassigned angular span(s) [13].

In this paper, we introduce an angle-optimized finite-difference time-domain (AO-FDTD) scheme aimed at controlling the angular sector of minimum dispersion error in three-dimensional (3-D) simulations. Because of the 3-D grid symmetry, the angle optimization occurs on each octant concurrently. Section II gives the implementation details and presents a stability analysis of the proposed 3-D AO-FDTD scheme. In Section III, we show how 3-D AO-FDTD can be used to precisely control the angle of minimum numerical dispersion. Numerical results are presented in Section IV.

Manuscript received December 14, 2002; revised October 24, 2002. This work was supported in part by the NRC under Contract CR-96-0013 and under an SBC/Ameritech Grant.

The authors are with the ElectroScience Laboratory and Department of Electrical Engineering, The Ohio State University, Columbus, OH 43212 USA (e-mail: wangs@ee.eng.ohio-state.edu).

Digital Object Identifier 10.1109/TMTT.2003.808615

II. Update Equations and Stability Analysis

We introduce a modified set of Maxwell's curl equations as follows:

$$([T]\cdot\nabla)\times\vec{E}=-\frac{\partial\vec{B}}{\partial t}$$
$$([T]\cdot\nabla)\times\vec{H}=\frac{\partial\vec{D}}{\partial t} \tag{1}$$

where $([T]\cdot\nabla)$ denotes the dot product of vector differential operator ∇ and an artificial correction tensor $[T]$ defined as

$$[T]=\begin{bmatrix}\alpha-\beta\dfrac{\Delta x^2\partial_t^2}{v_p^2} & 0 & 0\\ 0 & \alpha-\beta\dfrac{\Delta y^2\partial_t^2}{v_p^2} & 0\\ 0 & 0 & \alpha-\beta\dfrac{\Delta z^2\partial_t^2}{v_p^2}\end{bmatrix} \tag{2}$$

in which Δx, Δy, and Δz are the cell size along the x, y, and z directions respectively, $v_p=1/\sqrt{\mu\varepsilon}$ is the exact (continuum) phase velocity in the medium, and α and β are additional degrees of freedom in the equations. These parameters are to be determined in order to control phase-correcting (higher order) time derivative terms. This artificial correction tensor is designed so as to introduce artificial dispersion effects which compensate the numerical dispersion. The compensation mechanism will be detailed in Section III.

Second-order time derivatives terms can also be written in terms of the second-order space derivatives via the Helmholtz equation [14]. Thus, (2) becomes

$$[T]=\begin{bmatrix}\alpha-\beta\Delta x^2\nabla^2 & 0 & 0\\ 0 & \alpha-\beta\Delta y^2\nabla^2 & 0\\ 0 & 0 & \alpha-\beta\Delta z^2\nabla^2\end{bmatrix}. \tag{3}$$

Implementing (3) in the staggered FDTD grid with central differencing in space and a leap-frog discretization in time, we obtain fully discrete update equations for the 3-D AO-FDTD. For example, the E_x update is written as shown in the equation at the bottom of the following page, where the superscripts denote the spatial location of the field components and the subscripts denote the time step. The other update equations are similar. The AO-FDTD methodology can also be specialized for two-dimensional (2-D) simulations following a similar procedure. This is described in more detail elsewhere [15].

To investigate the stability of the 3-D AO-FDTD method, we employ a Von Neumann analysis [2]. The E and H fields are expanded into Fourier modes as

$$
\begin{aligned}
&E_{xi}^{l+(1/2),m,n} \\
&\quad = E_{xi}(t)\exp\left(-j\left[k_x\left(l+\tfrac{1}{2}\right)\Delta x + k_y m\Delta y + k_z n\Delta z\right]\right) \\
&E_{yi}^{l,m+(1/2),n} \\
&\quad = E_{y_i}(t)\exp\left(-j\left[k_x l\Delta x + k_y\left(m+\tfrac{1}{2}\right)\Delta y + k_z n\Delta z\right]\right) \\
&E_{zi}^{l,m,n+(1/2)} \\
&\quad = E_{zi}(t)\exp\left(-j\left[k_x l\Delta x + k_y m\Delta y + k_z\left(n+\tfrac{1}{2}\right)\Delta z\right]\right) \\
&H_{xi+(1/2)}^{l,m+(1/2),n+(1/2)} \\
&\quad = H_{xi+(1/2)}(t)\exp\left(-j\left[k_x l\Delta x + k_y\left(m+\tfrac{1}{2}\right)\Delta y\right.\right. \\
&\qquad\qquad \left.\left. + k_z\left(n+\tfrac{1}{2}\right)\Delta z\right]\right) \\
&H_{yi+(1/2)}^{l+(1/2),m,n+(1/2)} \\
&\quad = H_{yi+(1/2)}(t)\exp\left(-j\left[k_x\left(l+\tfrac{1}{2}\right)\Delta x + k_y m\Delta y\right.\right. \\
&\qquad\qquad \left.\left. + k_z\left(n+\tfrac{1}{2}\right)\Delta z\right]\right) \\
&H_{zi+(1/2)}^{l+(1/2),m+(1/2),n} \\
&\quad = H_{zi+(1/2)}(t)\exp\left(-j\left[k_x\left(l+\tfrac{1}{2}\right)\Delta x + k_y\left(m+\tfrac{1}{2}\right)\Delta y\right.\right. \\
&\qquad\qquad \left.\left. + k_z n\Delta z\right]\right). \qquad (4)
\end{aligned}
$$

Substituting (4) into the discrete update equations, we obtain the amplification matrix as shown in (5), at the bottom of the following page, where

$$
\xi = \frac{4\Delta t^2}{\mu\epsilon}, \quad \zeta = 2j\frac{\Delta t}{\epsilon}, \quad \gamma = 2j\frac{\Delta t}{\mu}
$$

$$
\begin{aligned}
C_{xy} = &\frac{1}{\Delta z}\left[\alpha+\beta\left(3+2\frac{\Delta z^2}{\Delta y^2}+2\frac{\Delta z^2}{\Delta x^2}\right)\right]\sin\left(\frac{k_z\Delta z}{2}\right) \\
&-\frac{\beta}{\Delta z}\left[\sin\left(\frac{3k_z\Delta z}{2}\right)+2\sin\left(\frac{k_z\Delta z}{2}\right)\right. \\
&\qquad\left.\cdot\left(\frac{\Delta z^2}{\Delta x^2}\cos(k_x\Delta x)+\frac{\Delta z^2}{\Delta y^2}\cos(k_y\Delta y)\right)\right] \qquad (6)
\end{aligned}
$$

$$
\begin{aligned}
C_{xz} = &\frac{1}{\Delta y}\left[\alpha+\beta\left(3+2\frac{\Delta y^2}{\Delta x^2}+2\frac{\Delta y^2}{\Delta z^2}\right)\right]\sin\left(\frac{k_y\Delta y}{2}\right) \\
&-\frac{\beta}{\Delta y}\left[\sin\left(\frac{3k_y\Delta y}{2}\right)+2\sin\left(\frac{k_y\Delta y}{2}\right)\right. \\
&\qquad\left.\cdot\left(\frac{\Delta y^2}{\Delta x^2}\cos(k_x\Delta x)+\frac{\Delta y^2}{\Delta z^2}\cos(k_z\Delta z)\right)\right] \qquad (7)
\end{aligned}
$$

$$
\begin{aligned}
C_{yz} = &\frac{1}{\Delta x}\left[\alpha+\beta\left(3+2\frac{\Delta x^2}{\Delta y^2}+2\frac{\Delta x^2}{\Delta z^2}\right)\right]\sin\left(\frac{k_x\Delta x}{2}\right) \\
&-\frac{\beta}{\Delta x}\left[\sin\left(\frac{3k_x\Delta x}{2}\right)+2\sin\left(\frac{k_x\Delta x}{2}\right)\right. \\
&\qquad\left.\cdot\left(\frac{\Delta x^2}{\Delta y^2}\cos(k_y\Delta y)+\frac{\Delta x^2}{\Delta z^2}\cos(k_z\Delta z)\right)\right]. \qquad (8)
\end{aligned}
$$

$$
\begin{aligned}
&E_{xi+1}^{l+(1/2),m,n} \\
&= E_{xi}^{l+(1/2),m,n} + \frac{\Delta t}{\epsilon\Delta y}\left\{\left[\alpha+\beta\left(3+2\frac{\Delta y^2}{\Delta x^2}+2\frac{\Delta y^2}{\Delta z^2}\right)\right]\left(H_{zi+(1/2)}^{l+(1/2),m+(1/2),n}-H_{zi+(1/2)}^{l+(1/2),m-(1/2),n}\right)\right. \\
&\quad -\beta\left[\frac{\Delta y^2}{\Delta x^2}\left(H_{zi+(1/2)}^{l+(3/2),m+(1/2),n}-H_{zi+(1/2)}^{l+(3/2),m-(1/2),n}+H_{zi+(1/2)}^{l-(1/2),m+(1/2),n}\right.\right. \\
&\qquad \left.-H_{zi+(1/2)}^{l-(1/2),m-(1/2),n}\right) \\
&\quad +\frac{\Delta y^2}{\Delta z^2}\left(H_{zi+(1/2)}^{l+(1/2),m+(1/2),n+1}-H_{zi+(1/2)}^{l+(1/2),m-(1/2),n+1}+H_{zi+(1/2)}^{l+(1/2),m+(1/2),n-1}\right. \\
&\qquad \left.-H_{zi+(1/2)}^{l+(1/2),m-(1/2),n-1}\right) \\
&\quad \left.\left.+\left(H_{zi+(1/2)}^{l+(1/2),m+(3/2),n}-H_{zi+(1/2)}^{l+(1/2),m-(3/2),n}\right)\right]\right\} \\
&-\frac{\Delta t}{\epsilon\Delta z}\left\{\left[\alpha+\beta\left(3+2\frac{\Delta z^2}{\Delta x^2}+2\frac{\Delta z^2}{\Delta y^2}\right)\right]\left(H_{yi+(1/2)}^{l+(1/2),m,n+(1/2)}-H_{yi+(1/2)}^{l+(1/2),m,n-(1/2)}\right)\right. \\
&\quad -\beta\left[\frac{\Delta z^2}{\Delta x^2}\left(H_{yi+(1/2)}^{l-(1/2),m,n+(1/2)}-H_{yi+(1/2)}^{l-(1/2),m,n-(1/2)}+H_{yi+(1/2)}^{l+(3/2),m,n+(1/2)}-H_{yi+(1/2)}^{l+(3/2),m,n-(1/2)}\right)\right. \\
&\qquad +\frac{\Delta z^2}{\Delta y^2}\left(H_{yi+(1/2)}^{l+(1/2),m-1,n+(1/2)}-H_{yi+(1/2)}^{l+(1/2),m-1,n-(1/2)}+H_{yi+(1/2)}^{l+(1/2),m+1,n+(1/2)}\right. \\
&\qquad\quad \left.\left.\left.-H_{yi+(1/2)}^{l+(1/2),m+1,n-(1/2)}\right)+\left(H_{yi+(1/2)}^{l+(1/2),m,n+(3/2)}-H_{yi+(1/2)}^{l+(1/2),m,n-(3/2)}\right)\right]\right\}
\end{aligned}
$$

The eigenvalues of the amplification matrix in (5) are

$$\lambda = 1 \quad \lambda = 1 - \frac{\Xi\xi \pm \sqrt{\Xi(\Xi\xi^2 - 4\xi)}}{2}$$

with

$$\Xi = C_{xy}^2 + C_{xz}^2 + C_{yz}^2.$$

For the algorithm to be stable, we require $|\lambda| \leq 1$. Thus

$$\Delta t \leq 1/(v_p\sqrt{\Xi}). \tag{9}$$

When $\alpha = 1$, $\beta = 0$, this reduces to the usual Courant condition. Considering $\Delta x = \Delta y = \Delta z = h$, the largest possible value of $|C_{xy}|$, $|C_{xz}|$, and $|C_{yz}|$ is $(\alpha + 12\beta)/h$. Thus

$$\Delta t \leq \frac{h}{\sqrt{3}v_p(\alpha + 12\beta)}. \tag{10}$$

III. Optimal Angle Selection

Assuming a monochromatic wave propagating in a uniform grid, then the time-dependent factors of (4) can be written as

$$\vec{E}_i(t) = \vec{\mathcal{E}}\, e^{j\omega(i\Delta t)} \quad \vec{H}_{i+(1/2)}(t) = \vec{\mathcal{H}} e^{j\omega(i+(1/2))\Delta t}. \tag{11}$$

Substituting (4) and (11) again into the update equations and eliminating all H field variables, we obtain (12), as shown at the bottom of this page, where

$$\tilde{C}_{xy} = C_{xy}\big|_{\substack{k_x = k\sin(\theta)\cos(\phi),\, k_y = k\sin(\theta)\sin(\phi),\\ k_z = k\cos(\theta),\, \Delta x = \Delta y = \Delta z = h}}$$

$$\tilde{C}_{xz} = C_{xz}\big|_{\substack{k_x = k\sin(\theta)\cos(\phi),\, k_y = k\sin(\theta)\sin(\phi),\\ k_z = k\cos(\theta),\, \Delta x = \Delta y = \Delta z = h}}$$

$$\tilde{C}_{yz} = C_{yz}\big|_{\substack{k_x = k\sin(\theta)\cos(\phi),\, k_y = k\sin(\theta)\sin(\phi),\\ k_z = k\cos(\theta),\, \Delta x = \Delta y = \Delta z = h}}.$$

and $k = \sqrt{k_x^2 + k_y^2 + k_z^2}$ and (θ, ϕ) are polar angles along which the wave propagates. For $\mathcal{E}_x$, $\mathcal{E}_y$, and $\mathcal{E}_z$ to admit nontrivial solutions, the determinant of the matrix in (12) must be zero. Thus, we obtain the dispersion relation

$$\left[\frac{\sqrt{3}}{\chi}\sin\left(\frac{\chi kh}{2\sqrt{3}}\right)\right]^2 = h^2(\tilde{C}_{xy}^2 + \tilde{C}_{xz}^2 + \tilde{C}_{yz}^2) \tag{13}$$

where $\chi = v_p\Delta t\sqrt{3}/h$ is the Courant (or CFL) number.

Note that in the derivation of (13) we have implicitly assumed $k = \omega/v_p$. Therefore, for given (θ, ϕ), and χ, the error on the discrete phase velocity can be made equal to zero if α and β are properly chosen. In other words, we one can solve for α and β using (13) for given (θ, ϕ), and χ. In order to do this, we first define an error measure

$$\delta = \left[\frac{\sqrt{3}}{\chi}\sin\left(\frac{\chi kh}{2\sqrt{3}}\right)\right]^2 - h^2\left(\tilde{C}_{xy}^2 + \tilde{C}_{xz}^2 + \tilde{C}_{yz}^2\right). \tag{14}$$

Solving (13) is equivalent to letting $\delta = 0$. By noting that $kh = 2\pi h/\lambda$, we may expand δ in a polynomial series in terms of the reciprocal of the number of cells per wavelength, $q = h/\lambda$, as

$$\delta = (1-\alpha^2)\pi^2q^2 + \frac{\pi^4q^4}{288}\left\{63\alpha^2 - 2304\alpha\beta - 32\chi^2 + 3\alpha^2 \cdot \left[4\cos(2\theta) + 7\cos(4\theta) + 8\cos(4\phi)\sin^4(\theta)\right]\right\} + \mathcal{O}(q^6) \tag{15}$$

where, in practice, usually $q \leq 0.1$. To solve for α and β, we force the first two terms in (15) to be zero. The resulting error will be $\mathcal{O}(q^6)$. We obtain $\alpha = 1$ and

$$\beta = \frac{63 - 32\chi^2 + 12\cos(2\theta) + 21\cos(4\theta) + 24\cos(4\phi)\sin^4(\theta)}{2304}. \tag{16}$$

For $0 \leq \beta < 1/24$, the minimum (for all angles) maximum χ for a stable scheme is found from (10) and (16) to be 2/3. This is the CFL number which can be used to minimize the dispersion

$$\begin{bmatrix} 1-\xi\left(C_{xy}^2+C_{xz}^2\right) & \xi C_{xz}C_{yz} & \xi C_{xy}C_{yz} & 0 & \zeta C_{xy} & -\zeta C_{xz} \\ \xi C_{xz}C_{yz} & 1-\xi\left(C_{xy}^2+C_{yz}^2\right) & \xi C_{xy}C_{xz} & -\zeta C_{xy} & 0 & \zeta C_{yz} \\ \xi C_{xy}C_{yz} & \xi C_{xy}C_{xz} & 1-\xi\left(C_{yz}^2+C_{xz}^2\right) & \zeta C_{xz} & -\zeta C_{yz} & 0 \\ 0 & -\gamma C_{xy} & \gamma C_{xz} & 1 & 0 & 0 \\ \gamma C_{xy} & 0 & -\gamma C_{yz} & 0 & 1 & 0 \\ -\gamma C_{xz} & \gamma C_{yz} & 0 & 0 & 0 & 1 \end{bmatrix} \tag{5}$$

$$\begin{bmatrix} \frac{\sin^2\left(\frac{\omega\Delta t}{2}\right)}{v_p^2\Delta t^2} - \tilde{C}_{xz}^2 - \tilde{C}_{xy}^2 & \tilde{C}_{xz}\tilde{C}_{yz} & \tilde{C}_{xy}\tilde{C}_{yz} \\ \tilde{C}_{xz}\tilde{C}_{yz} & \frac{\sin^2\left(\frac{\omega\Delta t}{2}\right)}{v_p^2\Delta t^2} - \tilde{C}_{xy}^2 - \tilde{C}_{yz}^2 & \tilde{C}_{xy}\tilde{C}_{xz} \\ \tilde{C}_{xy}\tilde{C}_{yz} & \tilde{C}_{xy}\tilde{C}_{xz} & \frac{\sin^2\left(\frac{\omega\Delta t}{2}\right)}{v_p^2\Delta t^2} - \tilde{C}_{xz}^2 - \tilde{C}_{yz}^2 \end{bmatrix} \begin{bmatrix} \mathcal{E}_x \\ \mathcal{E}_y \\ \mathcal{E}_z \end{bmatrix} = 0 \tag{12}$$

TABLE I
SOME COEFFICIENTS USED IN THE 3-D AO-FDTD

	Non-filtered	Butterworth $q_c = 0.1$	Butterworth $q_c = 0.09$	Butterworth $q_c = 0.08$
α	1	0.999319	0.999562	0.999732
β	0.0354938	0.0389119	0.0382103	0.0376044

TABLE II
COEFFICIENTS USED IN THE 3-D AO-FDTD WITH THE CHEBYSHEV FILTERING SCHEME. $\Delta q = 0.02$ FOR ALL CHEBYSHEV FILTERS

	Chebyshev $q_c = 0.1$	Chebyshev $q_c = 0.09$	Chebyshev $q_c = 0.08$
α	0.999368	0.999591	0.999748
β	0.0388736	0.0382207	0.0376482

error for *any* angle with guaranteed stability. The actual CFL number can be made larger than 2/3 depending on the specific α and β chosen. Note that the angular dependency on (θ, ϕ) only appears in β, which controls the higher order time derivative terms.

Narrow-band problems comprise just a small fraction of problems of interest for FDTD simulations. In most cases, one is confronted with simulations involving broad-band excitations. Therefore, the treatment of the dispersion error over some preassigned and possibly broad frequency range is also of interest. In order to achieve that, we note that monomials $\{q^n\}$ in (15) can be thought of as a basis of an infinite dimensional linear space $\mathcal{P}_\infty[q]$ and (15) as an expansion of $\delta(q)$ in $\mathcal{P}_\infty[q]$. Therefore, we might as well choose another basis to expand (14), e.g., $\{(q-q_c)^n\}$ or $\{T_n[(q-q_c)/\Delta q]\}$, where q_c corresponds to a center frequency, Δq corresponds to the frequency range of interest, and $T_n(x)$ is the nth-order first-kind Chebyshev polynomial. In this manner, we are able to better control the frequency response of the dispersion error δ. The first alternative corresponds to a maximally flat (Butterworth) filter and the second one to a Chebyshev filter around the central frequency. After expanding the error in the new basis, the new α and β can then be determined by again forcing the lowest two terms of the expansion on the new basis to be identically zero. The implementation of such filters for finite-difference schemes is discussed in more detail in [16]. The improvement achieved using such filters is illustrated in the next section.

Although not detailed here, the modification on the dispersion behavior of Maxwell's equations given by (1) may also be effected, in a dual formulation, in terms of a change on the constitutive parameters of the background medium. In this dual formulation, Maxwell's equations themselves are not changed, while the background medium becomes a dispersive and anisotropic medium. This is because: 1) the change of the spatial nabla operators in (1) is equivalent to a change on the metric of space [17], [18] and 2) a change on the metric can be recast as a change on the constitutive parameters [19] (the latter fact follows from the metric invariance of Maxwell's equations [20]). This is best appreciated using the language of differential forms (exterior calculus) for the electromagnetic fields [18], [20]. The dispersive and anisotropic properties of the artificial background media is such that they approximately compensate for the dispersion and anisotropy caused by the discretization.

IV. NUMERICAL EXPERIMENTS

For a particular choice of α and β in (2), the actual phase velocity v_p of AO-FDTD simulations can be obtained as a function of frequency and propagation angle directly from (13), as traditionally done in FDTD dispersion analysis. In this way, the 3-D AO-FDTD will be compared with the traditional FDTD method (Yee's scheme) and a particular scheme with second-order accuracy in time and fourth-order accuracy in space [$(2,4)$ scheme] [4]. Butterworth, Chebyshev, and nonfiltered AO-FDTD schemes are tested at $\theta = 90°$ and $\phi = 0°$ (i.e., positive x direction), with $\chi = 2/3$. Moreover, the results are normalized to $c = 1/\sqrt{\mu\epsilon}$. $\chi = 1$ is used for

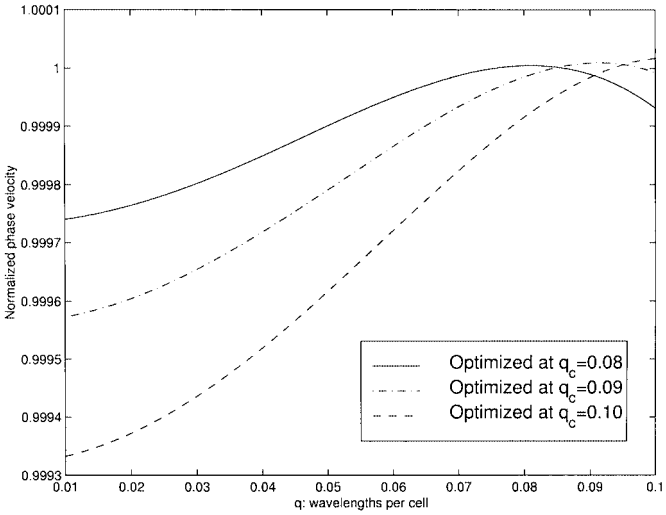

Fig. 1. Normalized phase velocity of the Butterworth AO-FDTD scheme at $\theta = 90°$ and $\phi = 0°$ with different specifications of center frequencies.

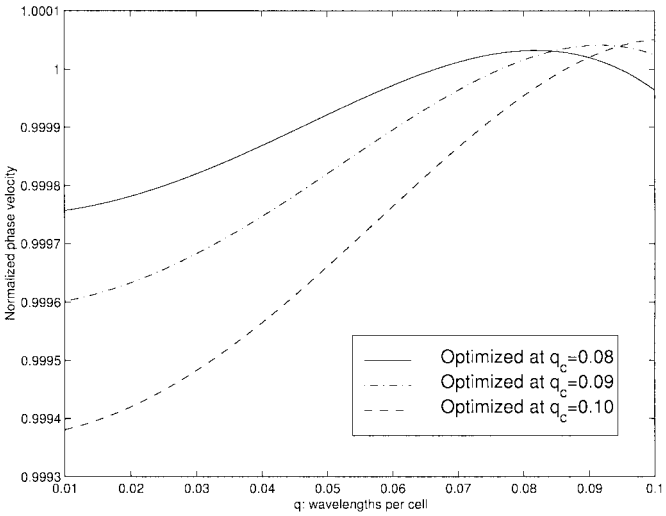

Fig. 2. Normalized phase velocity of the Chebyshev AO-FDTD scheme at $\theta = 90°$ and $\phi = 0°$ with different specifications of center frequencies.

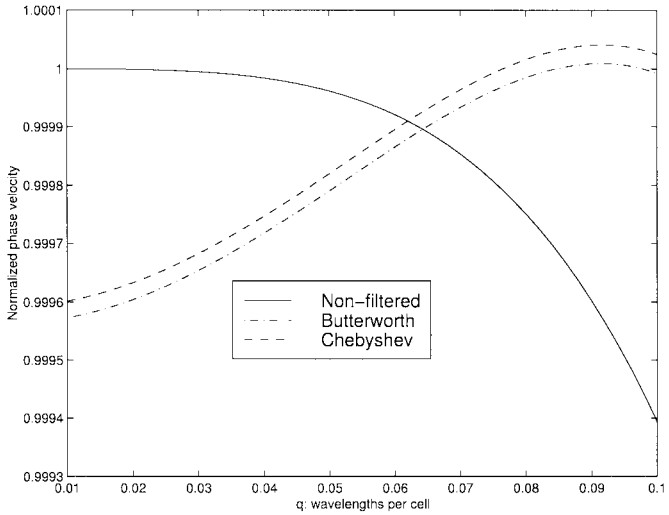

Fig. 3. Normalized phase velocity of Butterworth, Chebyshev, and nonfiltered AO-FDTD schemes at $\theta = 90^\circ$ and $\phi = 0^\circ$. For the filtered schemes, the center frequency is such that $q_c = 0.09$.

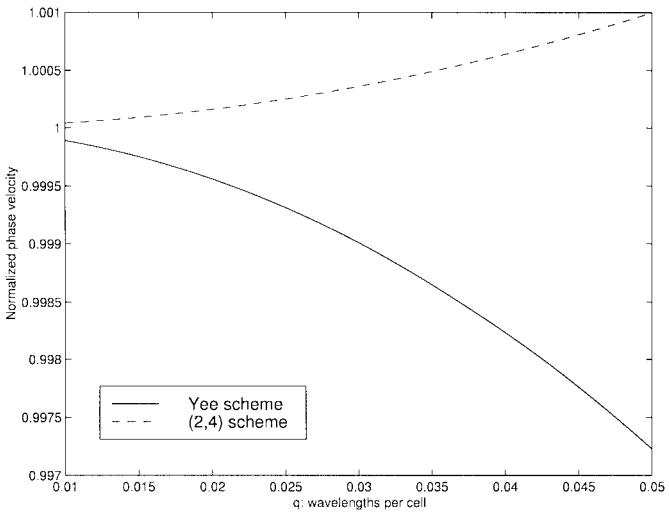

Fig. 4. Normalized phase velocity of ordinary FDTD and $(2,4)$ schemes at $\theta = 90^\circ$ and $\phi = 0^\circ$.

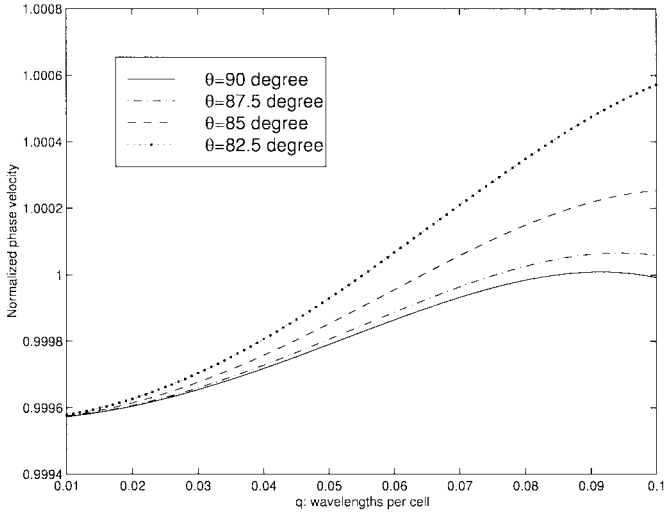

Fig. 5. Comparison of the normalized phase velocity at different angles of the Butterworth AO-FDTD scheme. The center frequency is such that $q_c = 0.09$.

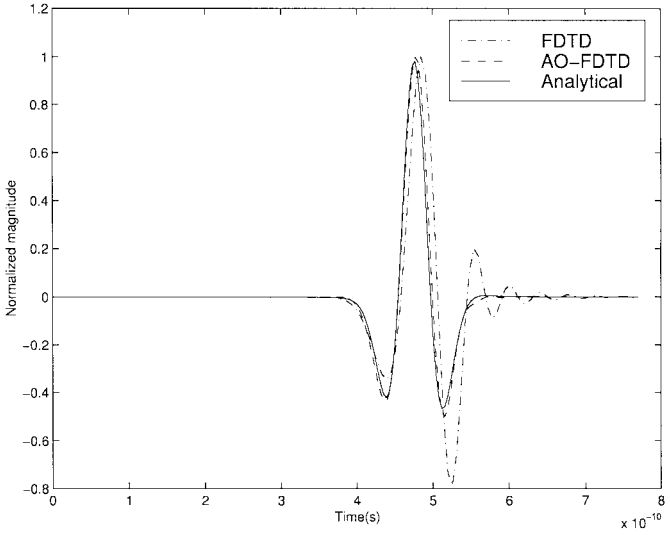

Fig. 6. Simulated results of a first-order differentiated Gaussian pulse propagating at $\theta = 90^\circ$ and $\phi = 0^\circ$.

ordinary FDTD and $\chi = 6/7$ for the $(2,4)$ scheme (maximum respective CFL numbers). The coefficients used here are listed in Tables I and II.

Figs. 1 and 2 show the normalized phase velocity of Butterworth and Chebyshev AO-FDTD schemes at $\theta = 90^\circ$ and $\phi = 0^\circ$ with different specificationof of center frequencies. The results are similar for these two schemes. In consonance with filter theory [21], we observe that the Butterworth filter gives slightly more accurate results than the Chebyshev filter at the specified center frequencies, while the Chebyshev filter produces a smaller maximum error than the Butterworth filter in the frequency band shown, $0.01 \leq q \leq 0.1$ (and indeed not limited to $\Delta q = 0.02$ from the filter specification).

Note that, in Fig. 1, the normalized phase velocities are not exactly 1.0 at the center frequencies, and this discrepancy tends to increase as the center frequency increases. This is because we are using a finite number of terms in the transformation of basis from q^n to $\{(q - q_c)^n\}$. Theoretically, this error could be minimized by increasing the number of terms when designing the filters. Alternatively, one can in practice simply shift the center frequency slightly downward (e.g., optimize at $q_c = 0.09$ instead of at $q_c = 0.1$).

An interesting point to observe in connection with Figs. 1 and 2 is that the local dispersion error is actually smaller for higher frequencies (closer to q_c) than for lower frequencies (as opposed to traditional FDTD schemes). This is highly desirable since at high frequencies the computational domain (of fixed physical size) is electrically larger than at low frequencies, and hence the *accumulated* phase error form the FDTD simulations is also larger. With this in mind, q_c may also be chosen close to the maximum frequency of interest.

Fig. 3 shows the comparison of different 3-D AO-FDTD schemes, where all filtering schemes are optimized with $q_c = 0.09$. We observe that filtering schemes indeed yield much better results than a nonfiltered scheme around designed frequencies, where the numerical dispersion is the most critical.

TABLE III
RATIOS OF MEMORY AND FLOP REQUIREMENTS OF YEE'S SCHEME VERSUS VARIOUS SCHEMES AT ($\theta = 90°$, $\phi = 0°$)

	Fang's (2,4)	Non-Filtered AO-FDTD	Butterworth AO-FDTD ($q_c = 0.09$)	Chebyshev AO-FDTD ($q_c = 0.09$)
Memory	3.2 (33)	4.3 (77)	7.3 (381)	8 (512)
FLOPs	2.8 (46)	1.3 (39)	3.7(328)	4.7(488)

Moreover, in the whole frequency range being considered, the maximum errors from both filtering schemes are also smaller than those of the nonfiltered scheme. Fig. 4 shows the normalized phase velocity of ordinary FDTD and $(2,4)$ schemes. Compared with the nonfiltered AO-FDTD scheme, approximately 5 times and 3 times finer meshes would be required for the same accuracy at $\theta = 90°$ and $\phi = 0°$, respectively. If compared with filtering schemes, even finer meshes would be required.

Fig. 5 illustrates the behavior of the dispersion error as a function of angle (anisotropy). A Butterworth filter optimized at $q_c = 0.09$ is used. The normalized phase velocity is presented for four different elevation angles close to the optimized angle $\theta_c = 90°$. The azimuthal angle is fixed at $\phi_c = 0°$. In the vicinity of the optimized angle, we see the 3-D AO-FDTD works as intended: an error no larger than 0.06% is obtained in an angular sector as large as 15° around the optimized angle. It is important to note here that, because of the symmetry of the 3-D Cartesian grid, the angle optimization occurs on each octant concurrently, i.e., the dispersion error is minimized (in general) at eight angles simultaneously. This can also be seen from the periodic behavior of β in (16) in terms of θ and ϕ. Exceptions to this occur for $\theta = 90°$, where the eight optimal propagation angles coalesce into four, and at $\theta = 0°$ or $\theta = 180°$, where the eight angles coalesce into only two.

We next simulate an ultrawide-band pulse propagation to illustrate the effectiveness of the angle optimization in reducing the pulse distortion caused by the numerical dispersion. The source is a $\hat{z}$-directed electric dipole excited by a first-order differentiated Gaussian pulse centered at 7.5 GHz and having -10 dB points at about 1.5 and 16 GHz. The medium is free-space and the computation domain is sufficiently large enough so that any spurious reflection from the grid boundaries are causally isolated from the results presented below. The discretization cell size corresponds to 10 cells per wavelength at 10 GHz. The observation point is at 38 cells away from the source at an angle $\theta = 90°$ and $\phi = 0°$, for which the optimization is chosen for the 3-D AO-FDTD. The copolarized component of the electric field at the observation point is illustrated in Fig. 6. The largest possible Courant numbers are used in each case, i.e., 1 for Yee's scheme and 2/3 for the AO-FDTD scheme. As a result of the much smaller numerical dispersion, the AO-FDTD pulse exhibits significantly less distortion than Yee's pulse.

Table III compares the relative amount of memory and floating point operations (FLOPs) required by Yee's scheme to obtain the same dispersion error at a given optimal angle of the AO-FDTD scheme, $\theta = 90°$ and $\phi = 0°$. For completeness, Fang's $(2,4)$ scheme is also considered. The largest possible Courant number is used within each scheme, and the same total elapsed time is assumed. The center frequency for the filtered schemes is chosen to be $q_c = 0.09$. We note that the amount of savings for filtered AO-FDTD methods depend on the specific frequency bandwidth of interest. At a single frequency, one can always fine tune the schemes using filters so that virtually no dispersion occurs at that particular frequency, and hence a direct comparison would indicate arbitrarily large savings. Hence, for a more meaningful comparison, we choose a frequency band and discretization cell size such that the lowest frequency corresponds to $\lambda/20$ and the highest frequency corresponds to $\lambda/10$.

Table III shows that, despite the need for (in general) smaller Courant numbers, and more arithmetic operation per field component update in the AO-FDTD and Fang's $(2,4)$ schemes, this is more than compensated for by the smaller number of grid points (large cell sizes) necessary for a given accuracy relative to Yee's grid. The main entries in this table correspond to a nonuniform Yee's grid, where the discretization cell size along the propagation direction is decreased with respect to the transversal directions, while the entries in parenthesis correspond to a uniform Yee's grid, where the cell size reduction occurs for all three directions simultaneously (note that the option of *independently* decreasing the cell size in a single direction for Yee's scheme can be used only for propagation angles strictly along the Cartesian axes). From this table, we see that, for example, to obtain the same dispersion error at this frequency range, a (nonuniform) Yee's scheme necessitates roughly eight times more memory and 4.7 times more FLOPs than the AO-FDTD scheme with a Chebyshev filter.

V. CONCLUSION

We have described conditionally stable, AO-FDTD algorithms which minimizes the dispersion error at preassigned propagation angles in 3-D problems. Because of the 3-D grid symmetry, the optimization occurs on each octant concurrently. The combination of the 3-D AO-FDTD with filtering schemes (Butterworth and Chebyshev) further improves the dispersion characteristics of a finite range of frequencies in the case of broad-band problems. This algorithm is of particular interest for electromagnetic field simulations in electrically large problems where the minimization of the dispersion error only around certain limited angular spans is critical, e.g., for highly elongated domains.

ACKNOWLEDGMENT

The authors gratefully acknowledge technical discussions with R. Lee and J.-F. Lee.

REFERENCES

[1] K. S. Yee, "Numerical solution of initial boundary value problems involving Maxwell's equation in isotropic media," *IEEE Trans. Antennas Propagat.*, vol. AP-14, pp. 302–307, Mar. 1966.

[2] A. Taflove, Ed., *Advances in Computational Electrodynamics: The Finite-Difference Time-Domain Method*. Norwood, MA: Artech House, 1998.

[3] J. B. Schneider and R. J. Kruhlak, "Dispersion of homogeneous and inhomogeneous waves in the Yee finite-difference time-domain grid," *IEEE Trans. Microwave Theory Tech.*, vol. 49, pp. 280–287, Feb. 2001.

[4] J. Fang, "Time domain computation for Maxwell's equations," Ph.D. dissertation, Univ. California at Berkeley, Berkeley, CA, 1989.

[5] T. Deveze, L. Beaulieu, and W. Tabbara, "A fourth order scheme for the FDTD algorithm applied to Maxwell's equations," in *Proc. IEEE AP-S Symp.*, vol. 1, 1992, pp. 346–349.

[6] M. F. Hadi and M. Piket-May, "A modified FDTD $(2,4)$ scheme for modeling electrically large structures with high-phase accuracy," *IEEE Trans. Antennas Propagat.*, vol. 45, pp. 254–264, Feb. 1997.

[7] J. B. Cole, "A high-accuracy realization of the Yee algorithm using nonstandard finite difference," *IEEE Trans. Microwave Theory Tech.*, vol. 45, pp. 991–996, June 1997.

[8] E. A. Forgy and W. C. Chew, "A new FDTD formulation with reduced dispersion for the simulation of wave propagation through inhomogeneous media," in *Proc. IEEE AP-S Symp.*, vol. 2, 1999, pp. 1316–1319.

[9] J. W. Nehrbass, J. O. Jević, and R. Lee, "Reducing the phase error for finite-difference methods without increasing the order," *IEEE Trans. Antennas Propagat.*, vol. 46, pp. 1194–1201, Aug. 1998.

[10] K. L. Shlager, J. G. Maloney, S. L. Ray, and A. F. Peterson, "Relative accuracy of several finite-difference time-domain methods in two and three dimensions," *IEEE Trans. Antennas Propagat.*, vol. 41, pp. 1732–1737, Dec. 1993.

[11] K. L. Shlager and J. B. Schneider, "Relative accuracy of several low-dispersion finite-difference time-domain schemes," in *Proc. IEEE AP-S Symp.*, vol. 1, 1999, pp. 168–171.

[12] T. Hirono, L. Wayne, S. Seki, and Y. Yoshikuni, "A three-dimensional fourth-order finite-difference time-domain scheme using a symplectic integrator propagator," *IEEE Trans. Microwave Theory Tech.*, vol. 49, pp. 1640–1648, Sept. 2001.

[13] S. Gedney, "The perfectly matched layer absorbing medium," in *Advances in Computational Electrodynamics: The Finite-Difference Time-Domain Method*, A. Taflove, Ed. Norwood, MA: Artech House, 1998.

[14] G. Cohen and P. Joly, "Fourth order schemes for the heterogeneous acoustics equation," *Comput. Methods Appl. Mech. Eng.*, vol. 80, no. 1–3, pp. 397–407, 1990.

[15] S. Wang and F. L. Teixeira, "A finite-difference time-domain algorithm optimized for arbitrary propagation angles," *IEEE Trans. Antennas Propagat.*, 2003, to be published.

[16] ——, "Dispersion-relation-preserving FDTD algorithms for large-scale three-dimensional problems," *IEEE Trans. Antennas Propagat.*, 2003, to be published.

[17] W. C. Chew and W. H. Weedon, "A 3D perfectly matched medium from modified Maxwell's equations with stretched coordinates," *Microwave Opt. Technol. Lett.*, vol. 7, no. 13, pp. 599–604, 1994.

[18] F. L. Teixeira and W. C. Chew, "Differential forms, metrics, and the reflectionless absorption of electromagnetic waves," *J. Electromagn. Waves Applicat.*, vol. 13, no. 5, pp. 665–686, 1999.

[19] ——, "General closed-form PML constitutive tensors to match arbitrary bianisotropic and dispersive linear media," *IEEE Microwave Guided Wave Lett.*, vol. 8, pp. 223–225, June 1998.

[20] ——, "Lattice electromagnetic theory from a topological viewpoint," *J. Math. Phys.*, vol. 40, no. 1, pp. 169–187, 1999.

[21] D. M. Pozar, *Microwave Engineering*. New York: Wiley, 1998.

Shumin Wang received the B.S. degree in physics from Qingdao University, Qingdao, R.O.C., in 1995, the M.S. degree in electronics from Beijing University, Beijing, China, in 1998, and is currently working toward the Ph.D. degree in electrical engineering at The Ohio State University, Columbus.

Since 1999, he has been a Graduate Research Associate with the ElectroScience Laboratory (ESL), The Ohio State University. His research interests include electrostatic and magnetostatic lens design, time-domain differential equation-based methods, and high-frequency asymptotic methods and their applications to scattering, packaging, microwave circuits, and antenna analysis.

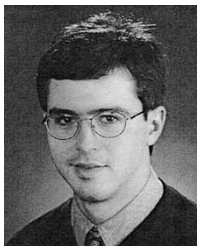

Fernando L. Teixeira received the B.S. and M.S. degrees in electrical engineering from the Pontifical Catholic University of Rio de Janeiro (PUC-Rio), Rio de Janeiro, Brazil, in 1991 and 1995, respectively, and the Ph.D. degree in electrical engineering from the University of Illinois at Urbana-Champaign, in 1999.

From 1999 to 2000, he was a Post-Doctoral Research Associate with the Research Laboratory of Electronics, Massachusetts Institute of Technology (MIT), Cambridge. Since 2000, he has been an Assistant Professor with the ElectroScience Laboratory (ESL) and the Department of Electrical Engineering, The Ohio State University, Columbus. His current research interests include analytical and numerical techniques for wave propagation and scattering problems in communication, sensing, and devices applications. He edited *Geometric Methods for Computational Electromagnetics* (Cambridge, MA: EMW, 2001), and has authored or coauthored over 30 journal papers and 50 conference papers in those areas.

Dr. Teixeira is a member of Phi Kappa Phi. He was the Technical Program Coordinator of the Progress in Electromagnetics Research Symposium (PIERS), Cambridge, MA, 2000. He was the recipient of the Raj Mittra Outstanding Research Award presented by the University of Illinois and a 1998 IEEE Microwave Theory and Techniques Society (IEEE MTT-S) Graduate Fellowship Award. He was the recipient of paper awards presented at the 1999 USNC/URSI National Radio Science Meeting, Boulder, CO, and at the 1999 IEEE Antennas and Propagation Society (IEEE AP-S) International Symposium, Orlando, FL. He was also the recipient of a Young Scientist Award presented at the 2002 URSI General Assembly.